

A. F. QASRAWI\*<sup>1</sup>, N. M. GASANLY<sup>2</sup>

<sup>1</sup>Faculty of Engineering, Atılım University, Ankara, Turkey.

<sup>2</sup>Department of Physics, Middle East Technical University, Ankara, Turkey.

## Carrier Transport Properties of InS Single Crystals

The electrical resistivity and Hall effect of indium sulfide single crystals are measured in the temperature range from 25 to 350 K. The donor energy levels located at 500, 40 and 10 meV below the conduction band are identified from both measurements. The data analysis of the temperature-dependent Hall effect measurements revealed a carrier effective mass of  $0.95 m_0$ , a carrier compensation ratio of 0.9 and an acoustic deformation potential of 6 eV. The Hall mobility data are analyzed assuming the carrier scattering by acoustic and polar optical phonons, and ionized impurities.

Keywords: InS crystal, resistivity, mobility, acoustic, polar, scattering mechanism

(Received May 23, 2002; Accepted June 28, 2002)

### 1. Introduction

InS is a member of III-VI semiconductor group including GaS, GaSe and InSe layered crystals. Indium sulfide crystallizes in the orthorhombic structure (KABALKINA et al.; GASANLY, AYDINLI). In this crystal, the In atoms have a tetrahedral coordination (three S and one In atom), however, the two S atoms and one In atom are in one layer, whereas the third S atom is in the neighboring layer. For this reason, the crystal structure of InS could be considered as a three-dimensional network somewhat different than the layered structure of its counterparts. The III-VI compounds with these properties attracted recently considerable attention on account of its semiconducting nature and applications in opto-electronic devices, radiation detectors and electrical switching (SINGH et al., ADDUCI et al., MEKHTIEV et al.).

Literature concerning the preparation and physical properties of InS crystal is relatively rare due to the difficulty of growing large single crystals. Although the structural properties of the crystal are fairly well established (KABALKINA et al.), and there has been few reports on the electrical conductivity and optical absorption (TAKARABE et al. 1987; NISHINO, HAMAKAWA), –up to our knowledge– there are no completely analyzed reports that clarify the transport phenomena of the crystals under investigation.

In our previous publication (GASANLY, AYDINLI) we have reported the results of photoluminescence (PL) measurements of InS crystals in the temperature range of 8.5–293 K and observed three bands located at 605, 626 and 820 nm in the PL spectra. This study allowed us to suggest a simple energy diagram that explains the recombination process in the crystals.

In this work we report the results of dark electrical resistivity and Hall mobility measurements in InS crystals. These measurements allowed us to identify the impurity levels

---

\* corresponding author: atef\_qasrawi@atilim.edu.tr

and to determine the donor and acceptor impurity concentrations, the electron effective mass and the electron scattering mechanisms in the crystal studied.

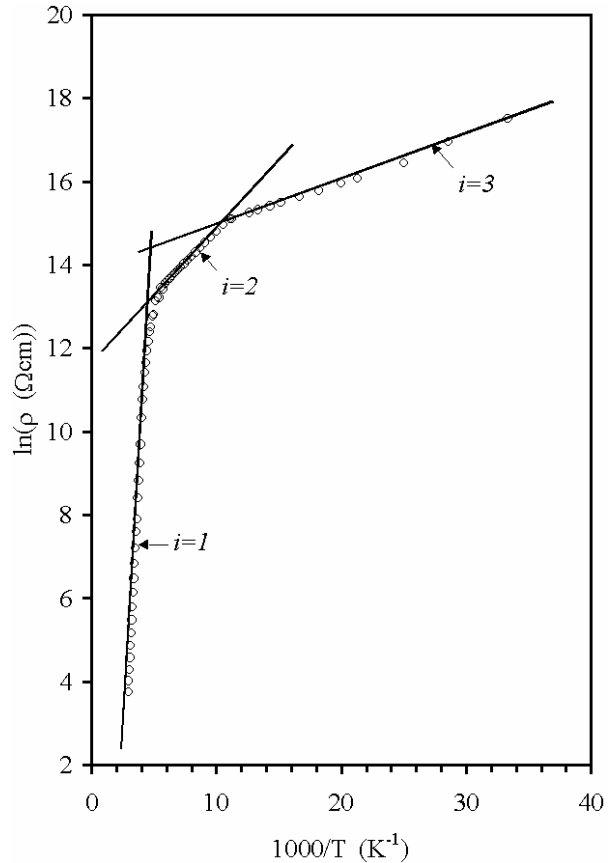


Fig. 1: The variation of dark electrical resistivity with temperature.

## 2. Experimental details

InS single crystals were grown by the modified Bridgman method using high purity (99.999%) elements taken in the stoichiometric proportions. Due to the fact that one of its three In-S bonds extends into neighboring layer, InS crystal has no distinct cleavage plane. Thus, samples suitable for measurements were obtained by hard cleavage along (100) plane perpendicular to the *c*-axis. Samples of  $3 \times 3 \times 1$  mm<sup>3</sup> size were used for the Hall effect measurements (HE). Ohmic contacts for HE measurements were made by soldering with high purity indium in the Van der Pauw configuration.

The Hall effect measurements were done in the temperature range 25-350 K in a closed cycle Lakeshore cryogenic system. The current flows along the layer, and the magnetic field (0.5 T) was applied perpendicular to it. The linearity in the Hall and ohmic voltages on the injected current was checked out at each temperature.

### 3. Results and Discussion

Both the hot probe technique and the sign of Hall coefficient ( $R_H$ ) indicate that the crystals exhibit  $n$ -type conduction. The ratio of the length to width of the samples is  $\sim 1.2$ , thus no corrections are made for the shortening effect of the current electrodes. The crystals exhibit a dark electrical resistivity ( $r$ ), Hall mobility ( $\mu$ ) and carrier concentration ( $n$ ) of  $4.6 \times 10^2 \Omega\text{cm}$ ,  $29 \text{ cm}^2\text{V}^{-1}\text{s}^{-1}$  and  $4.7 \times 10^{14} \text{ cm}^{-3}$  at room temperature, respectively. The values of the above reported electrical parameters are in good agreement with those reported for InS single crystals grown from the vapor phase by modified Bridgman method (ISMAILOV, KURBANOV). The value of  $r$  being greater, the carrier concentration and Hall mobility being lower than that reported for the crystals grown from indium melt (NISHINO, HAMAKAWA) may be attributed to the degree of disorder that arise from the difference in preparation techniques of the crystals.

To establish the dominant scattering mechanism in the samples, the temperature dependence of the resistivity and Hall mobility was examined in the temperature region of 25-350 K. General view of the resistivity as a function of reciprocal temperature is shown in Fig. 1. It was found that the resistivity increases with decreasing temperature, at higher rate in the high-temperature region (above 200 K). The variation of the resistivity with temperature is weak below 200 K.

The measured data of resistivity-temperature dependence are found to follow the relation,

$$r = r_{0i} \exp\left(\frac{E_{di}}{kT}\right), \quad (1)$$

where  $r_{0i}$  is the pre-exponential factor and  $E_{di}$  is the donor energy level in a specific temperature range (denoted by the letter  $i$ ). The values of  $E_{d1}$ ,  $E_{d2}$ , and  $E_{d3}$  calculated by using Eqn. (1) (see Fig. 1) were found to be 500, 37 and 10 meV in the temperature regions of 350-210 ( $i = 1$ ), 200-110 ( $i = 2$ ) and 100-25 K ( $i = 3$ ), respectively. The different values of  $E_{di}$  in different temperature regions indicate the extrinsic nature of conduction due to impurity carriers being located at different energy levels below the conduction band.

These impurity levels may be ascribed to the native structural defects such as In and/or S interstitial or vacancies and strain-induced defects, which may exist in InS crystals. The donor energy level being 10 meV coincides with the value determined from the PL measurements carried out on the crystals in our previous study (GASANLY, AYDINLI).

It is worth noting that, the fitting procedure was carried out by special high-convergence minimization program that uses the  $\chi^2$  method. The errors in the data were evaluated to be 2-10 %. Typical best fits to the experimental data are illustrated in Fig. 1.

The temperature dependence of carrier concentration,  $n$ , of InS crystals calculated from the relation  $n = 1/eR_H$  (the Hall factor has been assumed to be unity) is illustrated in Fig. 2. This figure shows the strong decrease of  $n$  from  $8.9 \times 10^{15} \text{ cm}^{-3}$  at 350 K to  $2.9 \times 10^{10} \text{ cm}^{-3}$  at 100 K. Below this temperature, the  $n-T$  variation is weak, indicating the degeneracy of carriers in the samples. Like the dark electrical resistivity, the carrier concentration exhibits an activated behavior with different activation energies in different temperature regions. For the samples under investigation, the carrier concentration activation energies calculated from

the slopes of the plot of  $\ln(n) - T^{-1}$  are found to be 504, 40 and 8 meV in the temperature regions of 350-210, 200-110 and 100-25 K, respectively. These values are approximately the same as those founded from the resistivity measurements. The reported activation energies suggest that electrons in InS are generated by the ionization of several donor levels whose origin was discussed before.

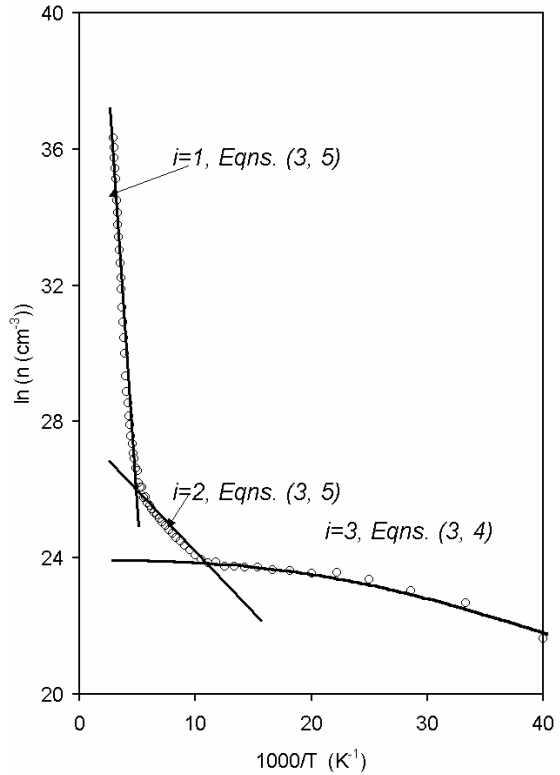


Fig. 2: Variation of carrier concentration with reciprocal temperature.

To get information about the carriers effective mass  $m^*$  and the impurity concentration present in the InS crystals, the temperature dependence of the carrier concentration was analyzed in details. To reveal the requested information the single donor-single acceptor model (being applied independently in each temperature range) was applied. The dependence of carrier concentration on temperature is given as (BLACKMORE),

$$\frac{n(n + N_a)}{N_{di} - N_a - n} = b N_c \exp\left(-\frac{E_{di}}{kT}\right), \tag{2}$$

where  $b$  is the degeneracy factor,  $N_c$  is the effective density of states of the conduction band,  $N_a$  and  $N_{di}$  are the acceptor and donor impurity concentrations presented in the crystals in a specific temperature region, respectively. Assuming both types of impurities to be present in the crystals and using the three-dimensional expression for  $N_c$ , the temperature dependence of  $n$  in Eqn. (2) could then be rewritten as,

$$n = \frac{2(N_{di} - N_a)}{1 + \frac{N_a}{bN_c} \exp(E_{di}/kT) + \left[ \left( 1 + \frac{N_a}{bN_c} \exp(E_{di}/kT) \right)^2 + \frac{4(N_{di} - N_a)}{bN_c} \exp(E_{di}/kT) \right]^{1/2}}. \quad (3)$$

By substituting the degeneracy factor  $b = 2$  and  $E_{d3} = 10$  meV, which is the value of donor ionization energy calculated from the resistivity and Hall measurements below 100 K, a computer numerical analysis was handled using Eqn. (3). The best fitting curve to the experimental data, obtained from the temperature-dependent Hall effect measurements in the range 100-25 K, is represented by the solid line in Fig. 2. As a result of this fitting procedure, data regressions provide the determination of the acceptor and donor concentrations in addition to the carrier effective mass ratio. The values of  $N_{d3} - N_a$ , and  $(m^*/m_0)$  were found to be  $2.5 \times 10^{10} \text{ cm}^{-3}$  and 0.95, respectively. The obtained value of  $(m^*/m_0) = 0.95$  is in good agreement with assumed value ( $m^* = m_0$ ) for the InS crystals in literature (NISHINO, HAMAKAWA; ISMAILOV, KURBANOV) where approximately similar behavior of mobility was observed in the crystals grown by different techniques. It should be noted that the solution obtained at low temperature from Eqn. (3) applies also for the heavy compensation condition where the carrier concentration takes the form (BLACKMORE),

$$n \approx \frac{(N_{d3} - N_a)}{1 + \left( \frac{N_a}{bN_c} \right) \exp(E_{d3}/kT)}. \quad (4)$$

Both Eqn. (3) and Eqn. (4) fit to the same data and illustrated by the coinciding solid lines in Fig. 2. The ratio  $N_a/N_{d3} \sim 0.9$  with  $N_{d3} = 3.2 \times 10^{17} \text{ cm}^{-3}$  suggests a large degree of compensation in the low temperature region (BLACKMORE).

In the moderate (210-100 K) and high (above 210 K) temperature regions Eqn. (3) is found to take the form (BLACKMORE),

$$n \approx bN_c \left( \frac{N_{di} - N_a}{N_a} \right) \exp\left(-E_{di}/kT\right). \quad (5)$$

The fitting of Eqn. (3) and Eqn. (5) with  $E_{d1} = 500$  meV and  $E_{d2} = 37$  meV reveals the values,  $(N_{d1} - N_a) = 3.9 \times 10^{19} \text{ cm}^{-3}$  and  $(N_{d2} - N_a) = 4.8 \times 10^{10} \text{ cm}^{-3}$  in the high and moderate temperature regions, respectively.

It should be noted that while handling the above analysis using Eqn. (3) the following considerations were taken into account:

- (1) The solutions of the above equations were controlled by the difference  $(N_{di} - N_a)$  with  $E_{di}$  taken from the resistivity curve.
- (2) Depending on the results obtained from PL spectra of the crystals (GASANLY, AYDINLI) the value of  $N_a$  was assumed to be the same at all temperatures.

(3) Eqn. (3) was solved in each temperature range independently from the other range.

(4) The fitting parameters obtained in the low temperature region were obtained in such a way that they fit the ionized impurity scattering mobility, as will be seen through the Hall mobility analysis.

The calculated parameters also provide an information about the ionized impurity concentration  $N_i$ . The values of  $N_i$  are found to be  $6.4 \times 10^{17}$ , and  $\sim 7 \times 10^{19} \text{ cm}^{-3}$  in the low and high temperature regions, respectively, for the samples under investigation. The calculated ionized impurity concentration is in good agreement with that obtained from the Hall mobility data reported for different samples of InS crystal (ISMAILOV, KURBANOV). The lack of information about the donor and acceptor levels and their related concentrations (ISMAILOV, KURBANOV) prevents us from comparing our results with others. However, the behavior of the carrier concentration of InS crystals with the fitting parameters  $E_{di}$ ,  $N_{di}$  and  $N_a$  may be compared with those reported for Sn-doped GaSe single crystals (*p*-type) where similar method of solution were applied for the *n*-*T* dependence (SANCHEZ-ROYO et al.). Different acceptor levels located at 310, 155 and 70 meV with  $N_{a1} = 2.7 \times 10^{16}$ ,  $N_{a2} = 2.7 \times 10^{16}$ ,  $N_{a3} = 1.7 \times 10^{15}$ , and  $N_d = 4 \times 10^{15} \text{ cm}^{-3}$  have been revealed for 0.2 at. % Sn doping GaSe crystals in the temperature regions of 400-300, 300-210 and 210-65 K, respectively.

The Hall mobility calculated from the relation  $\mathbf{m} = \mathbf{S} / ne$  was found to decrease with increasing temperature for  $T > 130 \text{ K}$ . In the narrow temperature region ( $130 \text{ K} < T < 100 \text{ K}$ ), the mobility variation with temperature is very slow. Below 100 K the mobility starts to decrease with decreasing temperature. The types of variation of  $\mathbf{m}$  in these temperature regions indicate that different scattering mechanisms dominate in these temperature regions. A logarithmic plot of  $\mathbf{m}T$  (see Fig. 3) in the high temperature region give a slope of ( $\sim -3/2$ ) which is an indication of thermal lattice scattering. In the low temperature region the plot of  $\ln(\mathbf{m}) - \ln(T)$  (Fig. 3) give a slope of ( $\sim 3/2$ ) that in turn indicates the domination of ionized impurity scattering mobility ( $\mathbf{m}$ ) for  $T < 100 \text{ K}$ . The temperature dependence of Hall mobility above 130 K could then be quantitatively interpreted using the scattering by polar optical phonons where the polar phonons mobility,  $\mathbf{m}_{po}$ , takes the form (WILEY),

$$\mathbf{m}_{po} = 25.4 \frac{T^{1/2}}{\mathbf{q}} \left( \frac{1}{\mathbf{e}_{\infty}} - \frac{1}{\mathbf{e}_s} \right)^{-1} \left( \frac{m_0}{m^*} \right)^{3/2} (e^z - 1) G(z). \text{ cm}^2 \text{ V}^{-1} \text{ s}^{-1}. \quad (6)$$

In this expression,  $\mathbf{e}_{\infty}$  and  $\mathbf{e}_s$  are the high-frequency and static dielectric constants, respectively,  $z = \mathbf{q} / T$ , where  $\mathbf{q}$  is the characteristic temperature of optical phonons,  $G(z)$  is a tabulated function,  $m^*$  is the effective mass of the carriers and  $m_0$  is the free electron mass. The values of  $\mathbf{e}_{\infty} = 9.7$  and  $\mathbf{e}_s = 22.5$  were determined using the infrared (IR) reflectivity data (TAKARABE et al 1983). The value of the characteristic temperature  $\mathbf{q} = 445 \text{ K}$  was calculated from the relation  $hcn = k\mathbf{q}$ , where  $\mathbf{n} = 309.5 \text{ cm}^{-1}$  is the frequency of the most intensive longitudinal optical mode observed through IR measurements (TAKARABE et al 1983). The polar phonons scattering mobility illustrated in Fig. 3 were calculated with no assumptions or extra fitting parameters. As could be seen from the figure the polar mobility values could not

fit the experimental data of Hall mobility in the high temperature region indicating the presence of other scattering mechanisms. Thus, the scattering by acoustic phonons was also taken into account. The acoustic phonons scattering mobility is given by the relation (WILEY),

$$\mathbf{m}_{ac} = 3.17 \times 10^{-5} \frac{du^2}{(m^*/m_0)^{5/2} E_{ac}^2 T^{3/2}}, \text{ cm}^2 \text{V}^{-1} \text{s}^{-1} \quad (7)$$

where  $d$  is the density in  $\text{g/cm}^3$ ,  $E_{ac}$  is the deformation potential in eV for acoustic phonons, and  $u$  is the average sound velocity which could be estimated from the formula,

$$u = \frac{k\mathbf{q}_D}{\hbar} \left( \frac{V}{6\rho^2} \right)^{1/3}. \text{ cm/s} \quad (8)$$

Here  $\mathbf{q}_D$  is the Debye temperature estimated by Lindemann's melting rule and  $V$  is the average atomic volume. In computing the acoustic phonons scattering mobility, the values of  $d$  and  $V$  were calculated as  $5.22 \text{ g/cm}^3$  and  $4.67 \times 10^{-23} \text{ cm}^3$ , respectively, using the x-ray results of the InS crystal that revealed an orthorhombic unit cell with lattice parameters of  $a = 3.944$ ,  $b = 4.447$  and  $c = 10.648 \text{ \AA}$  (KABALKINA et al.).  $\mathbf{q}_D$  was estimated as 195 K assuming a melting temperature of 1123 K (NISHINO et al.). Thus, the only remaining fitting parameter was the acoustic phonons deformation potential  $E_{ac}$ . The value of  $E_{ac} = 6 \text{ eV}$  was determined in such a way as to obtain the best fit between the experimental and the calculated polar combined with acoustic phonons scattering mobility in the high temperature region. The calculated acoustic deformation potential agrees well with that reported for  $\text{CuInSe}_2$  crystals where similar mobility behavior was observed (IRIE et al.).

The ionized impurity scattering mobility is given by the Brooks-Herring equation (WILEY). The temperature dependence of  $\mathbf{m}_i$  is calculated from

$$\mathbf{m}_i = \frac{3.28 \times 10^{15} \mathbf{e}_s^2 T^{3/2}}{(N_a + N_d) \left( m^*/m_0 \right)^{1/2} \left[ \ln(b+1) - \frac{b}{b+1} \right]} \quad (9)$$

where

$$b = \frac{1.29 \times 10^{14} \left( m^*/m_0 \right) \mathbf{e}_s T^2}{N^*}. \quad (10)$$

$N^*$  is the effective screening density and given by,

$$N^* = n + \frac{(n + N_a)(N_d - N_a - n)}{N_d}. \quad (11)$$

Using the values of  $N_d = N_{d3}$ ,  $N_a$ ,  $m^*/m_0$  and  $\mathbf{e}_s$ , the ionized impurity scattering mobility was calculated and illustrated in Fig. 3.

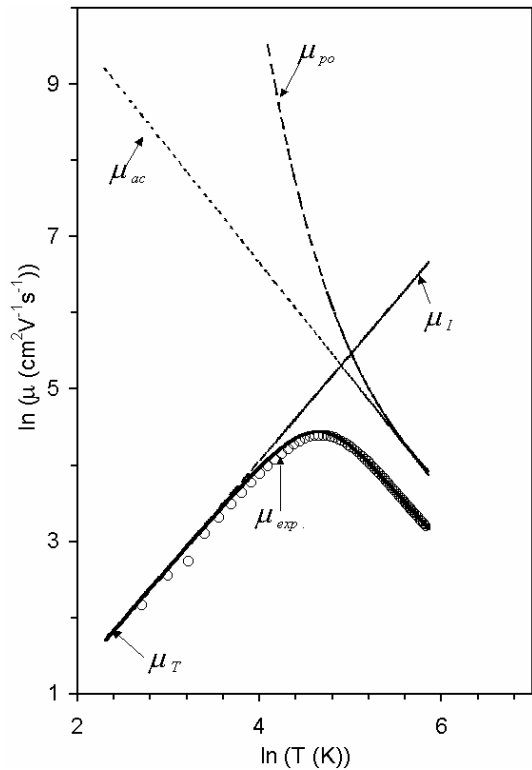


Fig. 3: Plot of  $\ln(\mu)$ - $\ln(T)$  for InS single crystals.

The ionized impurity scattering mobility, and the acoustic and polar phonons scattering mobilities are related to give the combined mobility  $m_T$  through the relation,

$$\frac{1}{m_T} = \frac{1}{m_{po}} + \frac{1}{m_{ac}} + \frac{1}{m_i} \tag{12}$$

Using Eqn. (12), the total mobility was evaluated and plotted in Fig. 3. The calculated theoretical  $m_T$  coincides with that obtained from the Hall effect experiments. Similar type of mobility behavior was reported for InS (ISMAILOV, KURBANOV),  $\text{CuIn}_5\text{S}_8$  (QASRAWI, GASANLY) and  $\text{CuInSe}_2$  (IRIE et al) single crystals. It should be noted that other solutions of the thermal lattice scattering mobility like electron-phonon scattering and scattering by non-polar phonons were not able to account for the mobility behavior of InS crystals. The first could fit the data with a very strong electron-phonon coupling constant of  $\sim 2$  which is usually observed in superconducting materials. The latter could not fit the data even for high non-polar deformation potential values.

### Conclusions

The electrical resistivity and Hall mobility of InS crystals are studied in the temperature range 25-350 K. Both measurements indicate the extrinsic *n*-type conductivity in all the

studied temperature range. The data analysis reveals three independent donor levels with energies of 500, 40 and 10 meV. The carrier effective mass being  $0.95 m_0$  with a compensation ratio of  $\sim 0.9$  and ionized impurity concentration of  $\sim 10^{19} - 10^{17} \text{ cm}^{-3}$  are determined from the single donor-single acceptor model. The Hall mobility data were analyzed assuming scattering due to acoustic combined with polar optical phonons at high temperatures and ionized impurities at low temperatures. The acoustic deformation potential being 6 eV determined for the conduction band is in good agreement with the values found in all IV and III-VI semiconductors.

### References

- ADDUCI, F. A., FERRARA, M., TANTALO, P., CINGOLANI, A., MINAFRA, A.: *Phys. Stat. Sol. (a)* **15** (1973) 303.
- BLACKMORE, S. K.: *Semiconductor Statistics*, Pergamon Press, New York (1962).
- GASANLY, N. M., AYDINLI, A.: *Sol. Stat. Commun.* **101** (1997) 797.
- IRIE, T., ENDO, S., KIMURA, S.: *Japan. J. Appl. Phys.* **18** (1979) 1303.
- ISMAILOV, I. M., KURBANOV, E. M.: *Sov. Phys. Journal* **32** (1989) 21.
- KABALKINA, S. S., LOSEV, V. G., GASANLY, N. M.: *Sol. Stat. Commun.* **44** (1982) 1383.
- MEKHTIEV, N. M., RUD, YU. V., SALAEV, E. YU.: *Sov. Phys. Semicond.* **12** (1978) 924.
- NISHINO, T., HAMAKAWA, Y.: *Japan. J. Appl. Phys.* **16** (1977) 1291.
- NISHINO, T., TAKAKURA, H., HAMAKAWA, Y.: *Japan. J. Appl. Phys.* **13** (1974) 1921.
- QASRAWI, A. F., GASANLY, N. M.: *Cryst. Res. Technol.* **36** (2001) 1399.
- SANCHEZ-ROYO, J. F., ERRANDONEA, D., SEGURA, A., ROA, L., CHEVY, A.: *J. Appl. Phys.* **83** (1998) 4750.
- SINGH, N. B., NARAYANAN, R., ZHAO, A. X., BALAKRISHNA, V., HOPKINS, R. H., SUHRE, D. R., FERNELIUS, N. C., HOPKINS, F. K., ZELMON, D. E.: *Mater. Sci. Eng. B* **49** (1977) 243.
- TAKARABE, K., KAWAMURA, H., WAKAMURA, K.: *Phys. Stat. Sol. (b)* **142** (1987) 605.
- TAKARABE, K., WAKAMURA, K., OGAWA, T.: *J. Phys. Soc. Japan* **52** (1983) 686.
- WILEY, J. D.: *Semiconductors and Semimetals* (Vol. 10), Academic Press, New York (1975).